

A mixed relaxed clock model. Supplementary material

Nicolas Lartillot¹, Matthew J Phillips², Fredrik Ronquist³.

¹ *Laboratoire de Biométrie et Biologie Evolutive, Lyon, France.*

`nicolas.lartillot@univ-lyon1.fr`

² *School of Earth, Environmental and Biological Sciences, Queensland University of Technology, Brisbane, Australia.*

`m9.phillips@qut.edu.au`

³ *Department of Biodiversity Informatics, Swedish Museum of Natural History, Box 50007, SE-104 05 Stockholm, Sweden.*

`fredrik.ronquist@nrm.se`

Running head: Mixed clock

Keywords: Molecular dating, Relaxed molecular clock, Bayesian inference, Monte Carlo.

Supplementary Tables

Table S1: Simulation results under the node-dating settings: true versus inferred proportion of variance contributed by the whitenoise component. Each pair of entries corresponds to a replicate simulated with parameter configurations drawn from the posterior distribution under the model indicated on the top line.

| BROWNIAN | | WHITENOISE | | MIXED | |
|----------|----------|------------|----------|-------|----------|
| true | inferred | true | inferred | true | inferred |
| 0% | 3% | 100% | 97% | 31% | 26% |
| 0% | 4% | 100% | 99% | 19% | 28% |
| 0% | 2% | 100% | 98% | 31% | 27% |
| 0% | 3% | 100% | 96% | 27% | 24% |
| 0% | 2% | 100% | 97% | 35% | 37% |
| 0% | 2% | 100% | 99% | 30% | 38% |
| 0% | 2% | 100% | 99% | 34% | 16% |
| 0% | 2% | 100% | 99% | 31% | 53% |
| 0% | 2% | 100% | 99% | 41% | 30% |
| 0% | 2% | 100% | 99% | 24% | 15% |

Table S2: Simulation results under the tip-dating settings: true versus inferred proportion of variance contributed by the whitenoise component. Each pair of entries corresponds to a replicate simulated with parameter configurations drawn from the posterior distribution under the model indicated on the top line, except for divergence times, which were drawn from the serial birth-death prior with diversified sampling.

| BROWNIAN | | WHITENOISE | | MIXED | |
|----------|----------|------------|----------|-------|----------|
| true | inferred | true | inferred | true | inferred |
| 0% | 3% | 100% | 99% | 47% | 40% |
| 0% | 3% | 100% | 99% | 40% | 31% |
| 0% | 4% | 100% | 99% | 38% | 71% |
| 0% | 2% | 100% | 99% | 42% | 64% |
| 0% | 3% | 100% | 98% | 37% | 60% |
| 0% | 3% | 100% | 99% | 50% | 60% |
| 0% | 5% | 100% | 99% | 45% | 55% |
| 0% | 5% | 100% | 98% | 47% | 38% |
| 0% | 12% | 100% | 99% | 36% | 43% |
| 0% | 8% | 100% | 99% | 35% | 52% |

Table S3: Simulation results under the tip-dating settings: true versus inferred proportion of variance contributed by the whitenoise component. Each pair of entries corresponds to a replicate simulated with parameter configurations drawn from the posterior distribution under the model indicated on the top line, except for divergence times, which were drawn from a serial Yule prior without diversified sampling.

| BROWNIAN | | WHITENOISE | | MIXED | |
|----------|----------|------------|----------|-------|----------|
| true | inferred | true | inferred | true | inferred |
| 0% | 13% | 100% | 99% | 47% | 85% |
| 0% | 13% | 100% | 99% | 40% | 98% |
| 0% | 58% | 100% | 99% | 38% | 87% |
| 0% | 27% | 100% | 99% | 42% | 71% |
| 0% | 20% | 100% | 99% | 37% | 90% |
| 0% | 13% | 100% | 99% | 50% | 68% |
| 0% | 41% | 100% | 99% | 45% | 78% |
| 0% | 17% | 100% | 99% | 47% | 38% |
| 0% | 14% | 100% | 99% | 36% | 65% |
| 0% | 20% | 100% | 98% | 35% | 81% |

Table S4: Simulation results under the tip-dating settings: true versus inferred proportion of variance contributed by the whitenoise component. Each pair of entries corresponds to a replicate simulated with parameter configurations drawn from the posterior distribution under the model indicated on the top line.

| BROWNIAN | | WHITENOISE | | MIXED | |
|----------|----------|------------|----------|-------|----------|
| true | inferred | true | inferred | true | inferred |
| 0% | 11% | 100% | 97% | 47% | 19% |
| 0% | 45% | 100% | 99% | 40% | 60% |
| 0% | 14% | 100% | 92% | 38% | 28% |
| 0% | 9% | 100% | 99% | 42% | 49% |
| 0% | 18% | 100% | 99% | 37% | 48% |
| 0% | 18% | 100% | 99% | 50% | 45% |
| 0% | 16% | 100% | 95% | 45% | 65% |
| 0% | 25% | 100% | 99% | 47% | 44% |
| 0% | 14% | 100% | 99% | 36% | 26% |
| 0% | 28% | 100% | 98% | 35% | 34% |

Table S5: Clade constraints used for estimating the tree topology for the tip-dating analysis.

| | |
|---------------------------------------|---|
| <i>Metacheiromys marshi</i> | stem Pangolin |
| <i>Moeritherium lyonsi</i> | stem Elephant |
| <i>Notharctus tenebrosus</i> | Primates (stem or crown) |
| <i>Dawsonolagus antiquus</i> | stem Lagomorpha (1) |
| <i>Gomphos elkema</i> | stem Lagomorpha (2, i.e. older than <i>Dawsonolagus</i>) |
| <i>Paramys delicatus</i> | stem Rodentia |
| <i>Cocomys lingchaensis</i> | stem Rodentia |
| <i>Tribosphenomys minutus</i> | stem Rodentia |
| <i>Rhombomylus turpanensis</i> | stem Glires or Lagomorpha or Rodentia |
| <i>Didolodus multicuspis</i> | stem Cetartiodactyla + Perissodactyla |
| <i>Thomashuxleya externa</i> | stem Cetartiodactyla + Perissodactyla |
| <i>Protolipterna ellipsodontoides</i> | stem Cetartiodactyla + Perissodactyla |
| <i>Carodnia vieirai</i> | stem Cetartiodactyla + Perissodactyla |

Table S5 (continued): Clade constraints used for estimating the tree topology for the tip-dating analysis.

| | |
|-----------------------------|--|
| Vulpavus ovatus | stem Carnivora |
| Vulpavus profectus | stem Carnivora |
| Sinopa rapax | stem Carnivora |
| Meshippus bairdi | stem Equidae |
| Basilosaurus cetoides | stem Cetacea (1) |
| Artiocetus clavis | stem Cetacea (2, i.e. older than Basilosaurus) |
| Rodhocetus balochistanensis | stem cetacea (3, i.e. older than Artiocetus) |
| Archaeotherium mortoni | stem Whippomorpha |
| Icaronycteris index | Chiroptera (stem or crown) |
| Onychonycteris finneyi | Chiroptera (stem or crown) |
| Hyopsodus paulus | Laurasiatheria (stem or crown) |
| Apheliscus insidiosus | Laurasiatheria (stem or crown) |
| Phenacodus intermedius | Laurasiatheria (stem or crown) |
| Mesonyx obtusidens | Laurasiatheria (stem or crown) |
| Protungulatum donnae | Laurasiatheria (stem or crown) |
| Leptictis dakotensis | stem Eutheria (1) |
| Ukhaatherium nessovi | stem Eutheria (2) |
| Zalambdalestes lechei | stem Eutheria (2) |
| Maelestes gobiensis | stem Eutheria (2) |
| Eomaia scansoria | stem Eutheria (3) |

Table S6: Fossil calibrations (My) used for the node-dating analysis. For each calibration, the calibrated node is referred to by two species, of which the node is the last common ancestor.

| Species 1 | Species 2 | Upper calibration | Lower calibration |
|-------------------------|-----------------------------|--------------------------|--------------------------|
| Cyclopes didactylus | Tamandua tetradactyla | 61.1 | 15.97 |
| Bradypus tridactylus | Choloepus sp. | 40.6 | 15.97 |
| Cyclopes didactylus | Choloepus sp. | 65.5 | 31.5 |
| Cyclopes didactylus | Dasypus novemcinctus | 71.2 | 58.5 |
| Dugong dugon | Trichechus manatus | 40.6 | 31.4 |
| Elephantulus rufescens | Rhynchocyon cirnei | 56 | 15.97 |
| Dugong dugon | Procavia capensis | 71.2 | 55.6 |
| Ochotona sp. | Oryctolagus cuniculus | 61.1 | 48.4 |
| Nycteris thebaica | Saccopteryx bilineata | 58.9 | 40.2 |
| Hipposideros commersoni | Rhinolophus creaghi | 56 | 37.1 |
| Megaderma lyra | Craseonycteris thonglongyai | 48.8 | 33.8 |
| Myotis lucifugus | Tadarida brasiliensis | 56 | 37.1 |
| Myotis lucifugus | Natalus stramineus | 61.1 | 48.4 |
| Pteronotus parnellii | Artibeus jamaicensis | 40.6 | 28.3 |
| Furipterus horrens | Noctilio sp. | 34 | 5.332 |
| Hipposideros commersoni | Myotis lucifugus | 61.1 | 48.4 |
| Canis lupus familiaris | Phoca vitulina | 56 | 37.1 |
| Ailuropoda melanoleuca | Phoca vitulina | 48.8 | 33.8 |
| Mephitis mephitis | Phoca vitulina | 48.8 | 33.8 |
| Procyon lotor | Meles meles | 40.6 | 27.6 |
| Procyon lotor | Mephitis mephitis | 40.6 | 30.9 |
| Felis silvestris | Prionodon linsang | 40.6 | 28.3 |
| Suricata suricatta | Canis lupus familiaris | 65.8 | 37.1 |

Table S6 (continued): Fossil calibrations (My) used for the node-dating analysis. For each calibration, the calibrated node is referred to by two species, of which the node is the last common ancestor.

| Species 1 | Species 2 | Upper calibration | Lower calibration |
|-----------------------------------|----------------------------|--------------------------|--------------------------|
| <i>Nycticebus coucang</i> | <i>Otolemur garnettii</i> | 56 | 37.1 |
| <i>Tarsius syrichta</i> | <i>Homo sapiens</i> | 58.9 | 37.1 |
| <i>Homo sapiens</i> | <i>Saimiri sciureus</i> | 56 | 28.3 |
| <i>Lemur catta catta</i> | <i>Otolemur garnettii</i> | 56 | 37.1 |
| <i>Tupaia glis</i> | <i>Ptilocercus lowii</i> | 65.8 | 37.1 |
| <i>Equus caballus</i> | <i>Tapirus indicus</i> | 61.1 | 55.5 |
| <i>Erinaceus europaeus</i> | <i>Sorex araneus</i> | 84.2 | 61.1 |
| <i>Erinaceus europaeus</i> | <i>Podogymnura truei</i> | 48.8 | 28.3 |
| <i>Lama glama</i> | <i>Tragulus napu</i> | 65.8 | 52.5 |
| <i>Sus scrofa</i> | <i>Pecari tajacu</i> | 37.3 | 15.97 |
| <i>Hippopotamus amphibius</i> | <i>Tursiops truncatus</i> | 61.1 | 52.5 |
| <i>Tursiops truncatus</i> | <i>Caperea marginata</i> | 48.8 | 33.8 |
| <i>Ictidomys tridecemlineatus</i> | <i>Aplodontia rufa</i> | 58.9 | 45.7 |
| <i>Ictidomys tridecemlineatus</i> | Gliridae | 61.1 | 48.4 |
| <i>Dinomys branickii</i> | <i>Chinchilla lanigera</i> | 37.3 | 24.5 |
| <i>Cavia porcellus</i> | <i>Dasyprocta punctata</i> | 37.3 | 24.5 |
| <i>Anomalurus beecrofti</i> | <i>Pedetes</i> sp. | 56 | 37.1 |
| <i>Hystrix</i> sp. | <i>Cavia porcellus</i> | 56 | 33.8 |
| Geomyidae | <i>Dipodomys heermanni</i> | 40.6 | 31.4 |
| <i>Dipodomys heermanni</i> | <i>Castor canadensis</i> | 61.1 | 52.4 |
| <i>Spalax</i> sp. | <i>Jaculus jaculus</i> | 58.9 | 45 |
| <i>Laonastes aenigmamus</i> | <i>Ctenodactylus gundi</i> | 48.8 | 28.3 |
| <i>Ictidomys tridecemlineatus</i> | <i>Hystrix</i> sp. | 65.8 | 55.6 |
| <i>Pedetes</i> sp. | <i>Castor canadensis</i> | 65.8 | 52.4 |

Table S7: Fossil age constraints (My) used for the tip-dating analysis.

| Species | Upper calibration | Lower calibration |
|---------------------------------------|--------------------------|--------------------------|
| <i>Eomaia scansoria</i> | 124.4 | 122.2 |
| <i>Maelestes gobiensis</i> | 83.6 | 72.1 |
| <i>Metacheiromys marshi</i> | 50.3 | 46.2 |
| <i>Ukhaatherium nessovi</i> | 83.6 | 72.1 |
| <i>Zalambdalestes lechei</i> | 83.6 | 72.1 |
| <i>Leptictis dakotensis</i> | 37.2 | 33.3 |
| <i>Moeritherium lyonsi</i> | 37.2 | 33.9 |
| <i>Notharctus tenebrosus</i> | 50.3 | 46.2 |
| <i>Protungulatum donnae</i> | 66.0 | 63.3 |
| <i>Apheliscus insidiosus</i> | 55.8 | 50.3 |
| <i>Phenacodus intermedius</i> | 56.8 | 55.8 |
| <i>Protolipterna ellipsodontoides</i> | 59.0 | 57.5 |
| <i>Hyopsodus paulus</i> | 50.3 | 46.2 |
| <i>Didolodus multicuspis</i> | 54.0 | 51.0 |
| <i>Carodnia vieirai</i> | 59.0 | 57.5 |
| <i>Thomashuxleya externa</i> | 54.0 | 51.0 |

Table S7 (continued): Fossil age constraints (My) used for the tip-dating analysis.

| Species | Upper calibration | Lower calibration |
|-----------------------------|--------------------------|--------------------------|
| Vulpavus ovatus | 50.3 | 46.2 |
| Vulpavus profectus | 50.4 | 46.2 |
| Sinopa rapax | 50.5 | 46.2 |
| Dawsonolagus antiquus | 54 | 53 |
| Gomphos elkema | 56 | 55 |
| Rhombomylus turpanensis | 54 | 53 |
| Tribosphenomys minutus | 59 | 57 |
| Paramys delicatus | 55.4 | 50.3 |
| Cocomys lingchaensis | 56 | 55 |
| Meshippus bairdi | 38.0 | 33.9 |
| Basilosaurus cetoides | 40.4 | 37.2 |
| Mesonyx obtusidens | 50.3 | 46.2 |
| Archaeotherium mortoni | 38.0 | 33.9 |
| Artiocetus clavis | 48.4 | 46 |
| Rodhocetus balochistanensis | 48.4 | 46 |
| Icaronycteris index | 52.5 | 50.3 |
| Onychonycteris finneyi | 52.5 | 50.3 |

Supplementary Figures

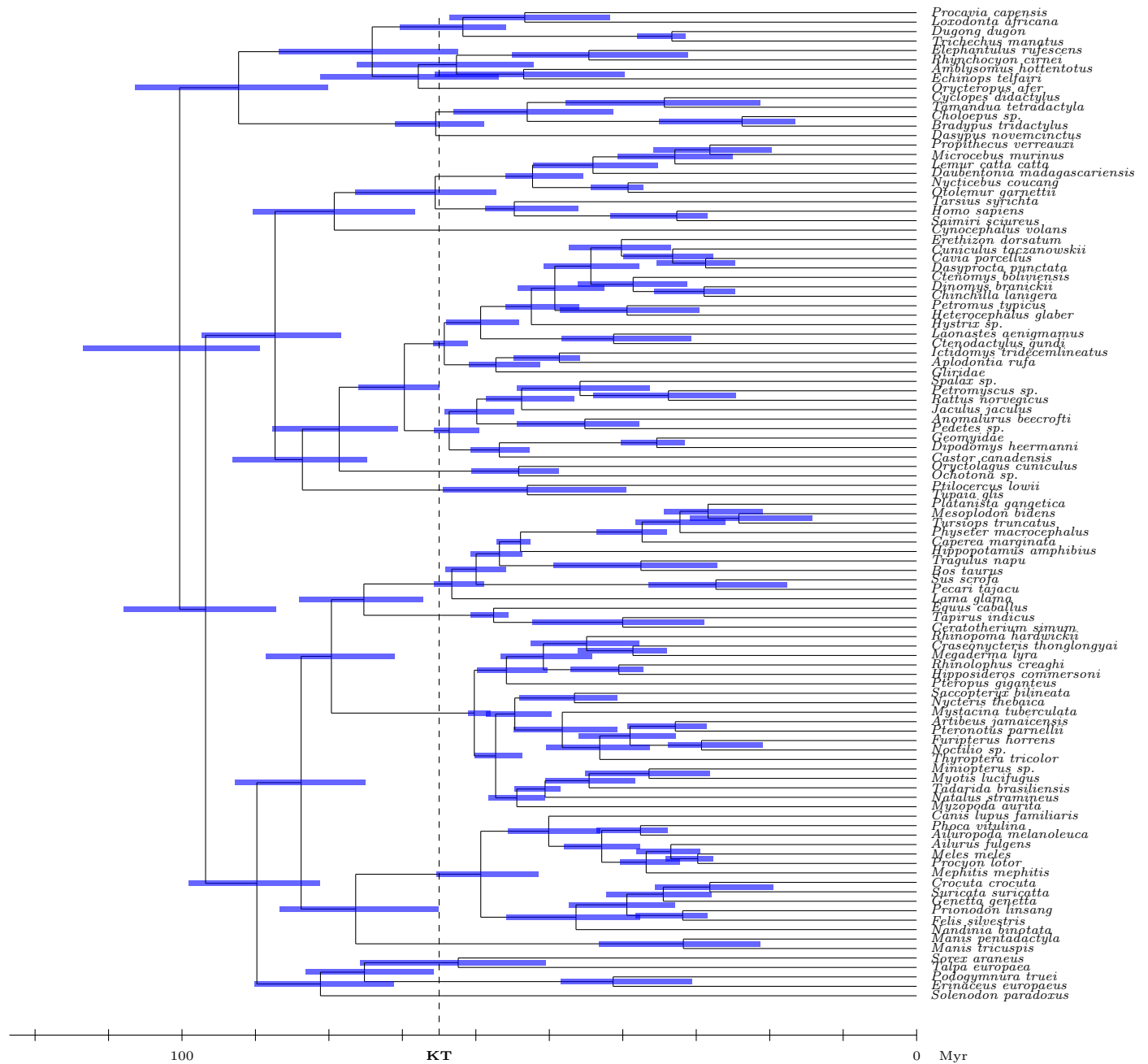


Figure S1. Inferred divergence times (posterior median, blue bars: 95% credible intervals) under the whitenoise clock, using the node-dating approach.

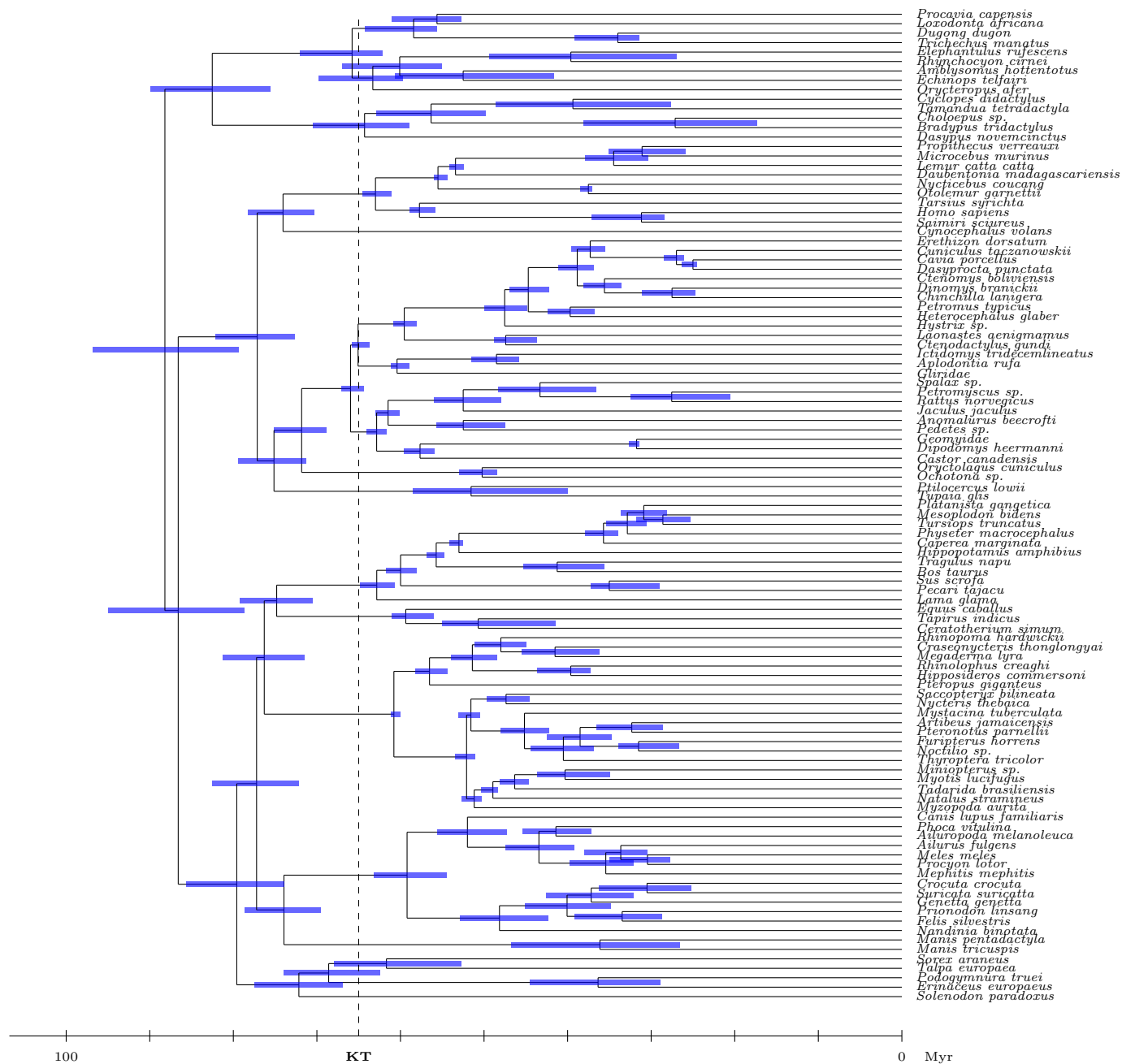


Figure S2. Inferred divergence times (posterior median, blue bars: 95% credible intervals) under the Brownian clock, using the node-dating approach.

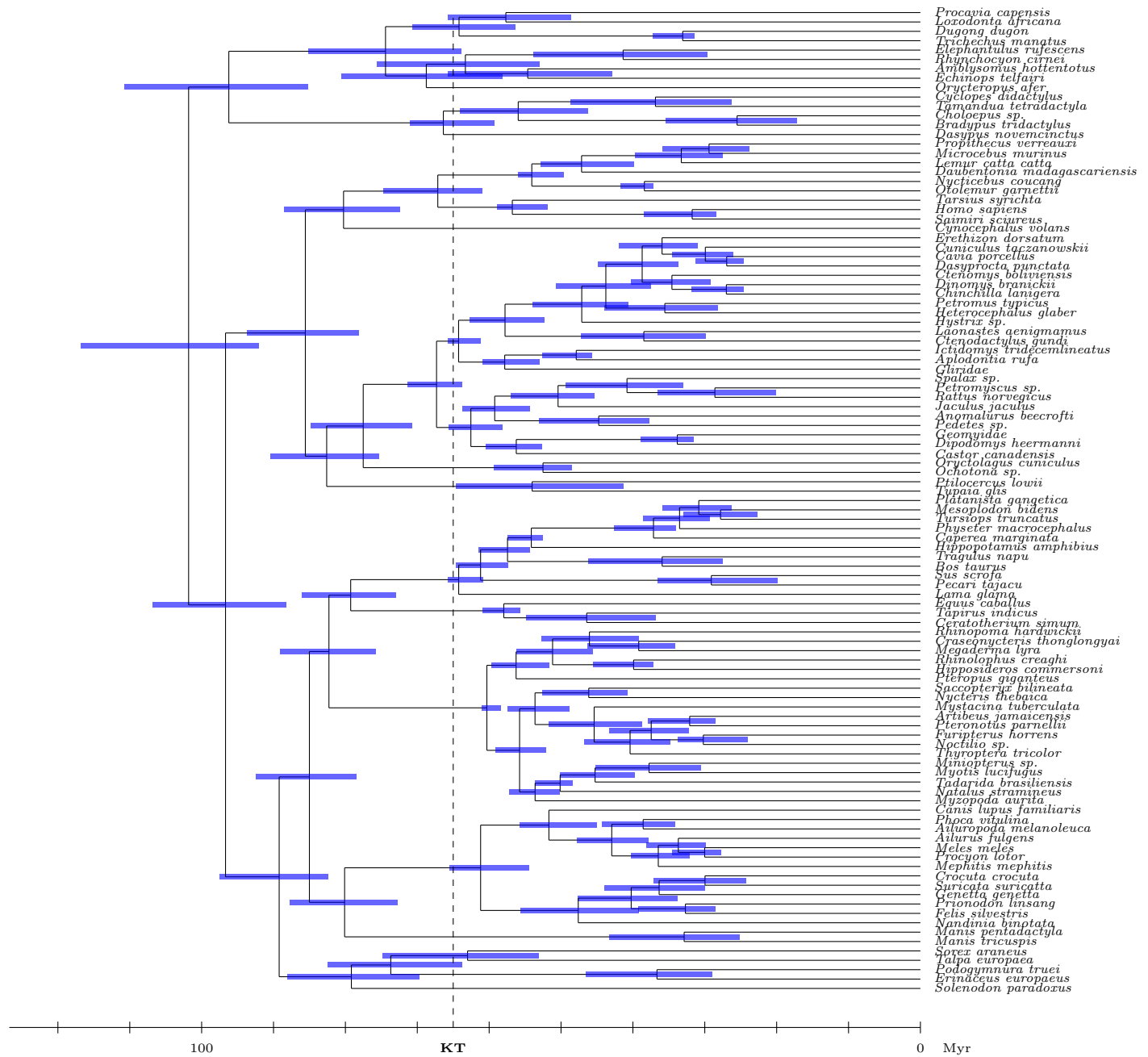


Figure S3. Inferred divergence times (posterior median, blue bars: 95% credible intervals) under the mixed clock, using the node-dating approach.

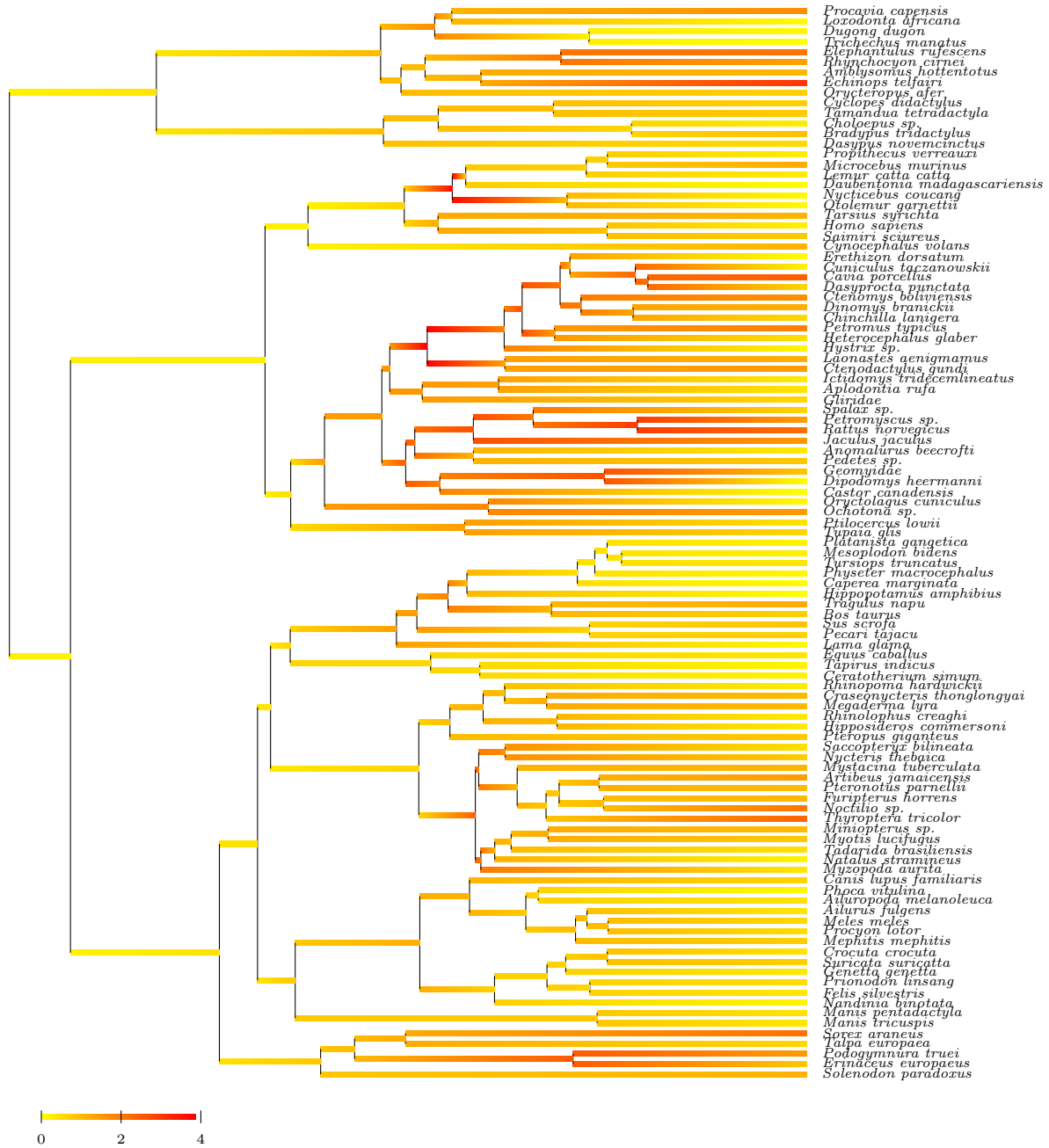


Figure S4. Inferred history of rate variation under the Brownian clock, using the node-dating approach.

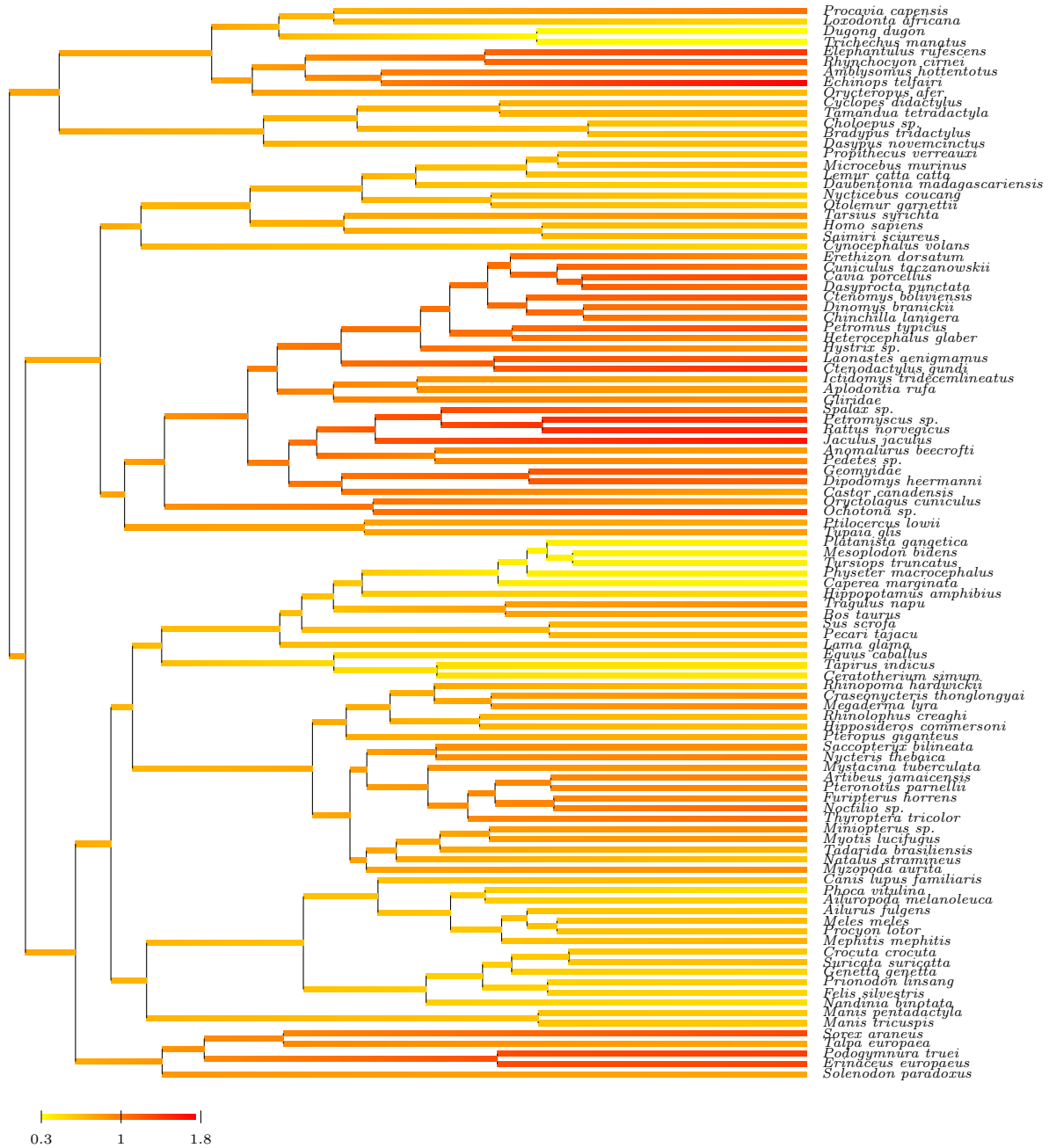


Figure S5. Inferred history of long-term rate variation (Brownian component of the mixed clock) using the node-dating approach.

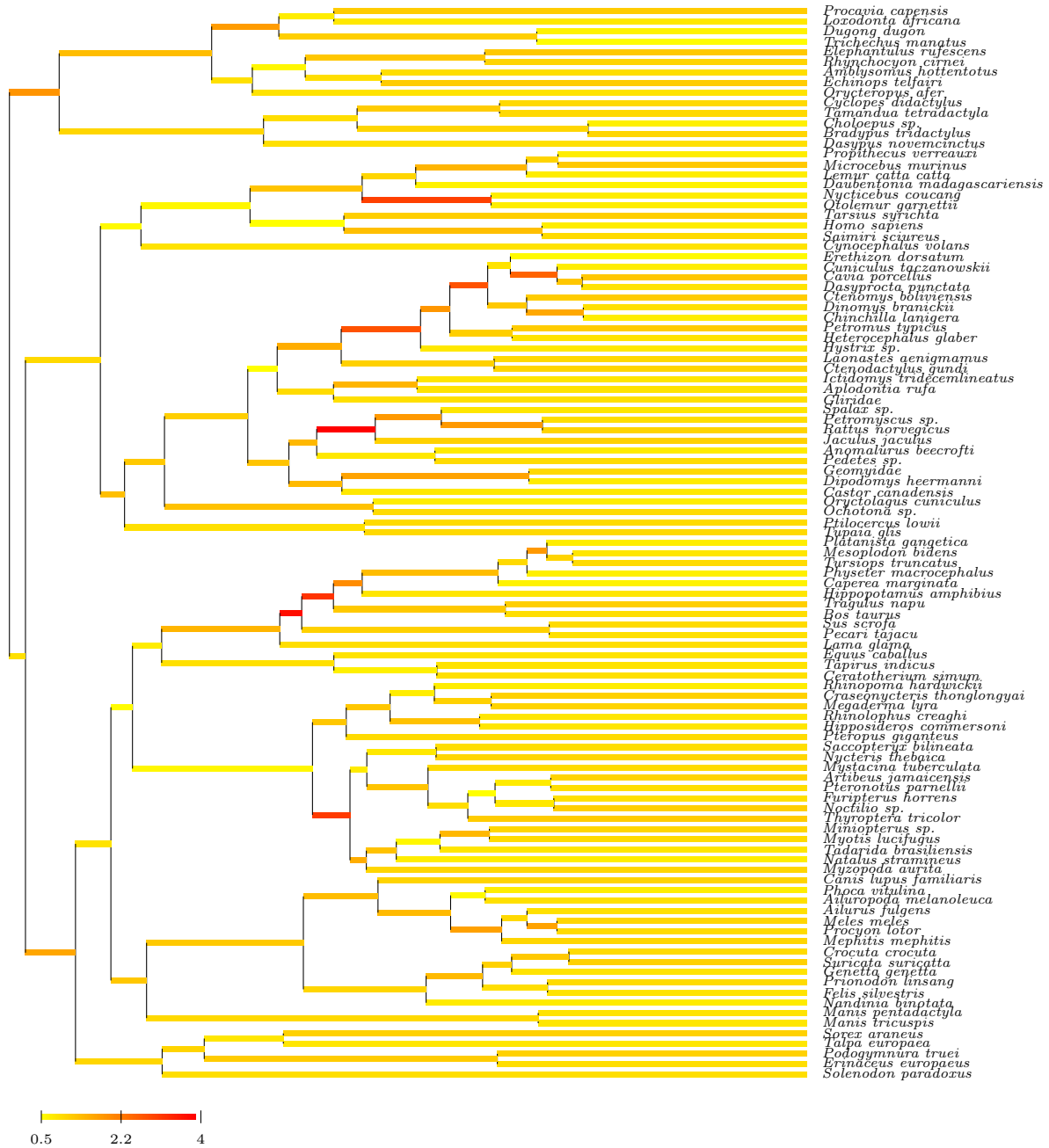


Figure S6. Inferred history of short-term rate variation (whitenoise component of the mixed clock) using the node-dating approach.

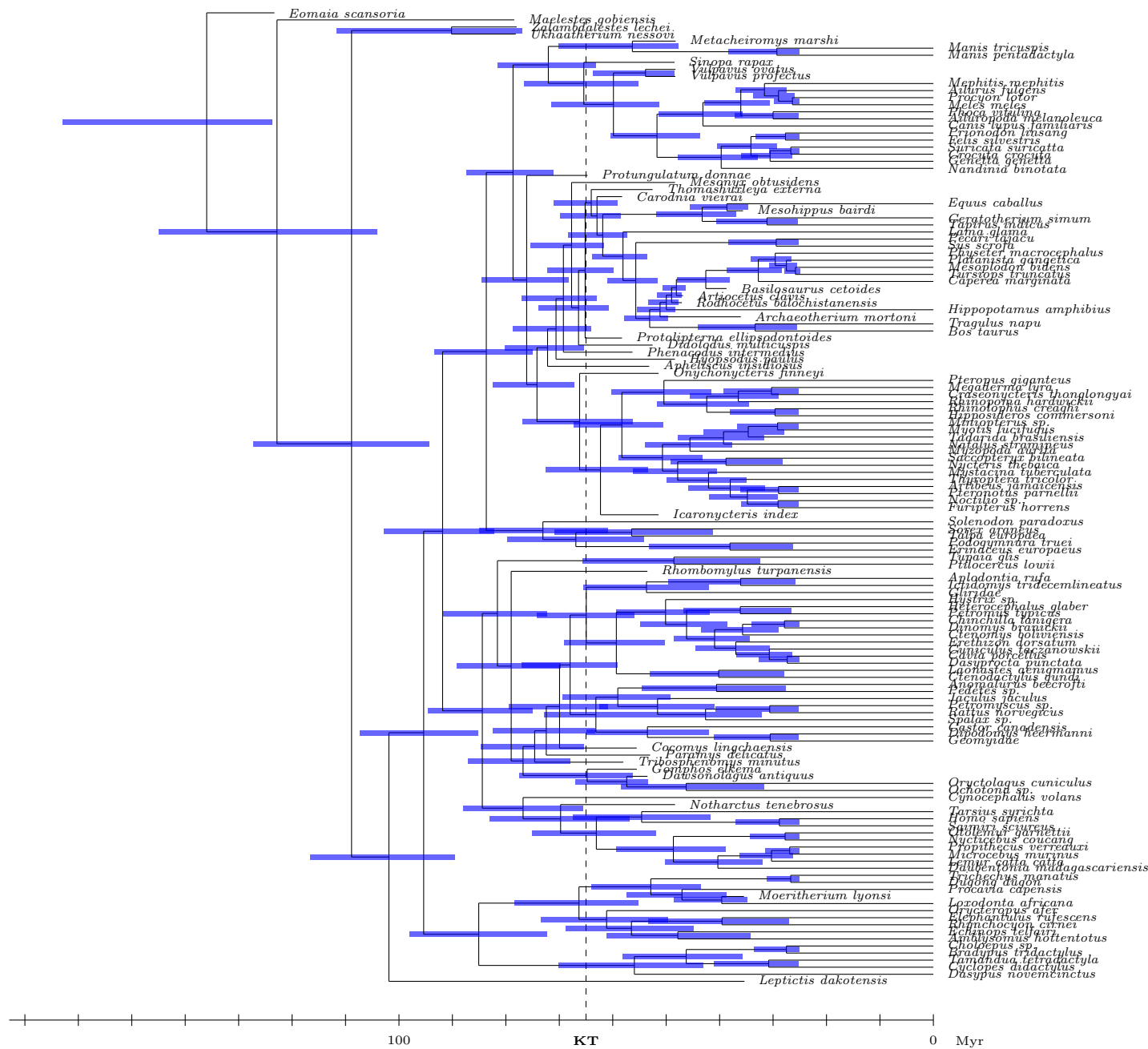


Figure S7. Inferred divergence times (posterior median, blue bars: 95% credible intervals) under the whitenoise clock, using the tip-dating approach.

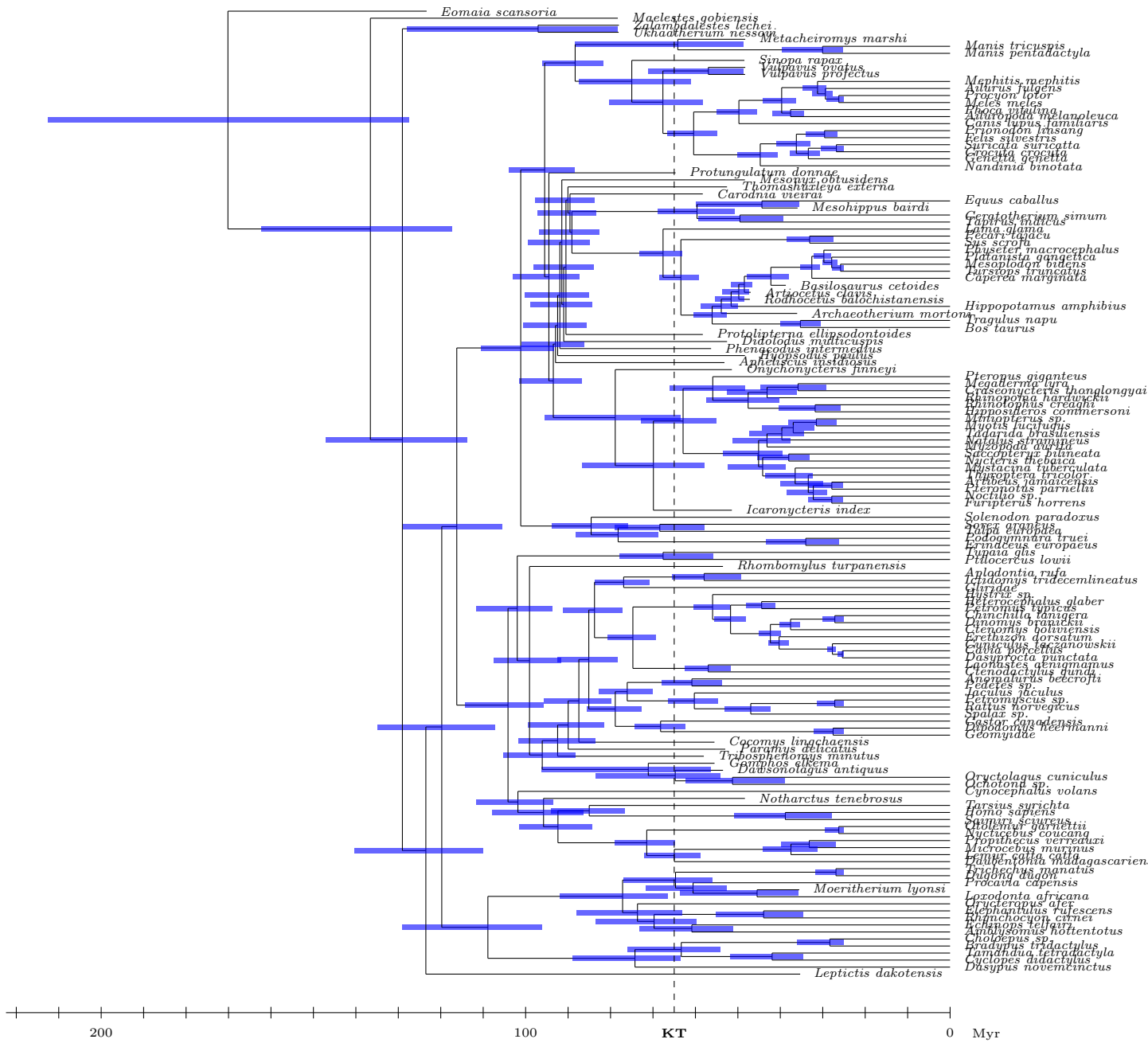


Figure S8. Inferred divergence times (posterior median, blue bars: 95% credible intervals) under the Brownian clock, using the tip-dating approach.

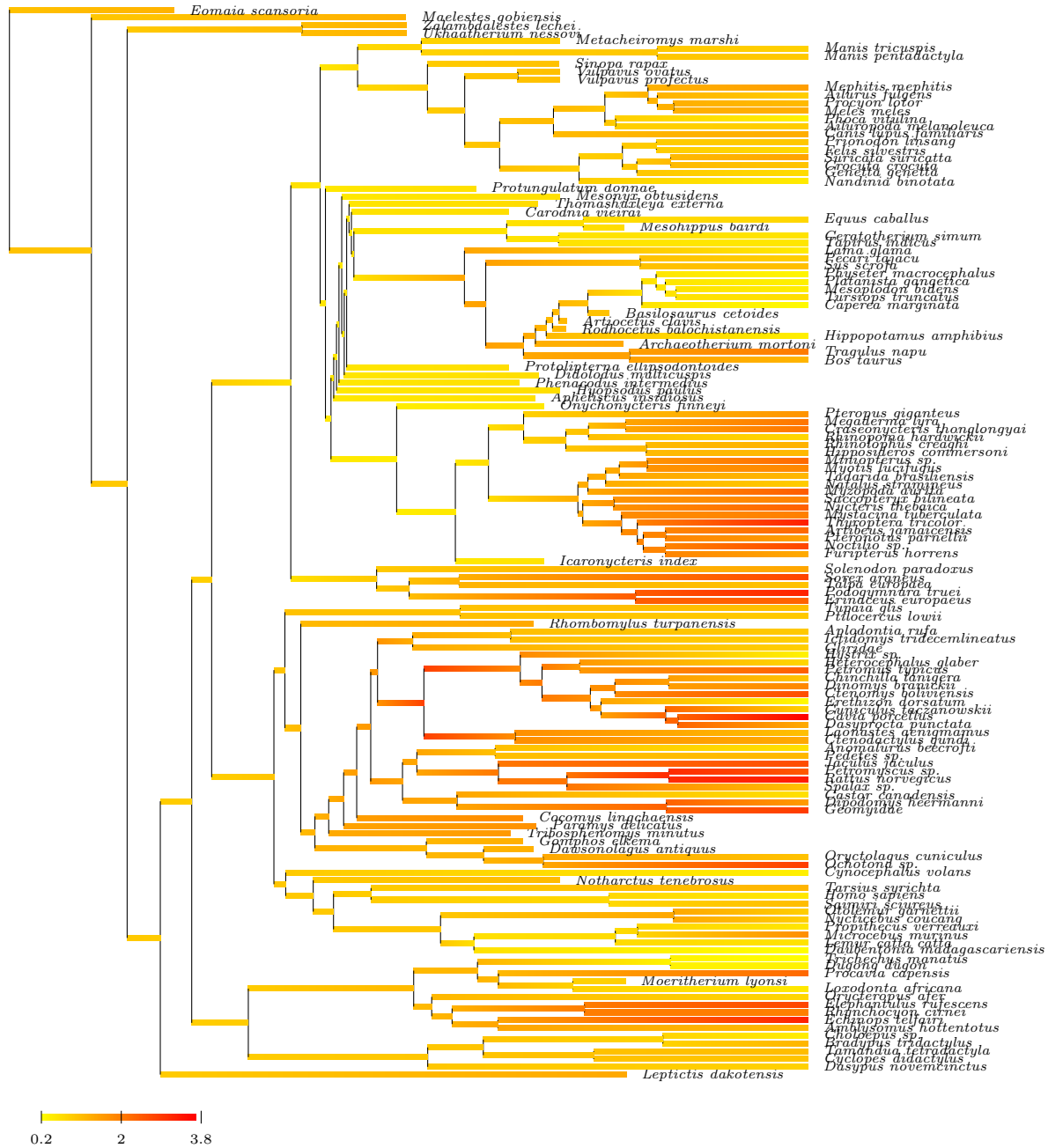


Figure S9. Inferred history of rate variation under the Brownian clock, using the tip-dating approach.

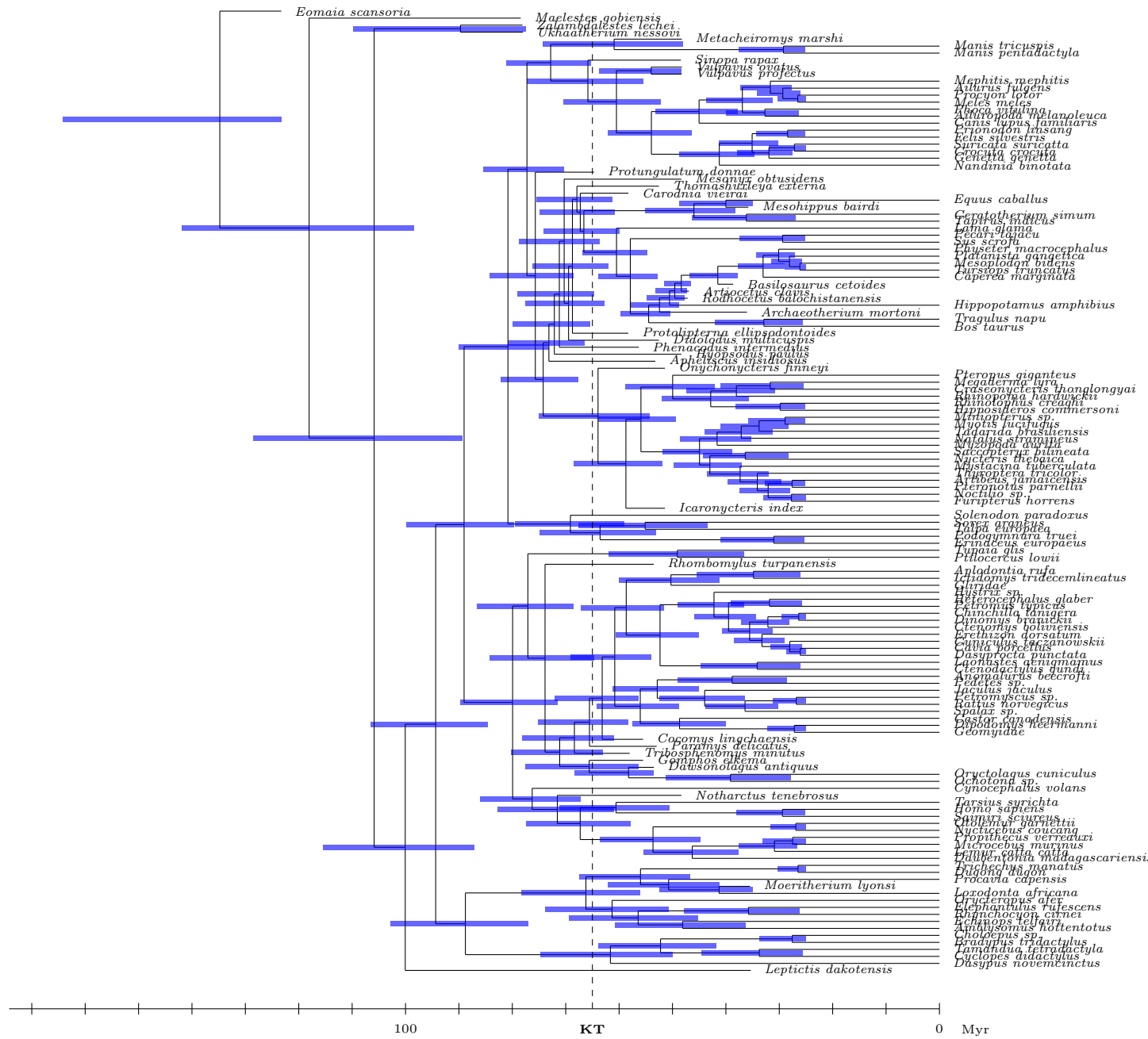


Figure S10. Inferred divergence times (posterior median, blue bars: 95% credible intervals)

under the mixed clock, using the tip-dating approach and with morphological characters.